

**Electronic Supplementary Information (ESI) for**

**Impact of a Conductive Oxide Core in Tungsten Sulfide-Based  
Nanostructures on the Hydrogen Evolution Reaction**

*Bora Seo,<sup>a</sup> Hu Young Jeong,<sup>b</sup> Sung You Hong,<sup>c</sup> Alla Zak,<sup>d</sup> and Sang Hoon Joo<sup>a,c\*</sup>*

<sup>a</sup>Department of Chemistry, Ulsan National Institute of Science and Technology (UNIST), 50 UNIST-gil, Ulsan 689-798, Republic of Korea.

<sup>b</sup>UNIST Central Research Facilities (UCRF), Ulsan National Institute of Science and Technology (UNIST), 50 UNIST-gil, Ulsan 689-798, Republic of Korea.

<sup>c</sup>School of Energy and Chemical Engineering, Ulsan National Institute of Science and Technology (UNIST), 50 UNIST-gil, Ulsan 689-798, Republic of Korea.

<sup>d</sup>Department of Sciences, Holon Institute of Technology (HIT), 52 Golomb St., Holon 5810201, Israel.

\*E-mail: shjoo@unist.ac.kr (S.H.J.)

## 1. Experimental Details

### 1.1. Synthesis of tungsten sulfide nanotubes (WS<sub>2</sub> NTs) and tungsten oxide/tungsten sulfide core-shell nanorods (W<sub>18</sub>O<sub>49</sub>@WS<sub>2</sub> NRs)

Inorganic nanotubes of tungsten disulfides were synthesized *via* the combined reduction-sulfidization process<sup>S1</sup> from tungsten oxide (WO<sub>x</sub>) by the solid-gas reaction with hydrogen (H<sub>2</sub>) and hydrogen sulfide (H<sub>2</sub>S) at elevated temperatures of 840 °C over 6 h. The quartz reactor used in this synthesis was designed specifically for this process. The detailed growth mechanism of the nanotubes in this reaction has been recently elucidated.<sup>S2</sup> The reaction mechanisms consists of two steps, namely growth of the oxide whiskers, and subsequent sulfidization, under the flow of H<sub>2</sub>S/H<sub>2</sub>. In the first step of the mechanism, the spherical nanoparticle (NP) precursors of tungsten oxide (WO<sub>x</sub>) grow into oxide whiskers of approximately 5-50 μm length and 20-120 nm diameter (Figure S1). The whiskers subsequently undergo sulfidization in the second step, resulting in formation of WS<sub>2</sub> nanotubes. These oxide whiskers grow as a result of partial reduction of the oxide precursor NPs and formation of a volatile suboxide phase, which serves as a building material for one-dimensional crystal synthesis. The growth of the whiskers results in the formation of a stable W<sub>18</sub>O<sub>49</sub> (WO<sub>2.72</sub>) phase, and followed by sulfidization. A fast reaction of H<sub>2</sub>S with the oxide nanowhiskers leads to the quick formation of a number of cylindrical closed WS<sub>2</sub> layers encapsulating the oxide core. A slow diffusion-controlled reaction then leads to full replacement of the oxygen atoms with sulfur atoms, and subsequently to the synthesis of the hollow WS<sub>2</sub>-NTs. In this study, partially and fully sulfidized WS<sub>2</sub> nanotubes were prepared. In order to obtain the partially sulfidized nanotubes (actually, nanorods with few sulfide layers and an oxide core, denoted as W<sub>18</sub>O<sub>49</sub>@WS<sub>2</sub> NRs), the reaction was stopped in the early stages.

### 1.2. Characterization Methods

Scanning electron microscopy (SEM) analysis was conducted on a field emission scanning electron microscope (Nanonova 230, FEI). High-resolution transmission electron microscopy (TEM) images were taken using a low-voltage spherical aberration (Cs)-corrected TEM (FEI Titan<sup>3</sup> G2 60-300) with an acceleration voltage of 80 kV. Energy dispersive spectroscopy (EDS) elemental mapping analyses were performed using a JEOL JEM 2100F with a probe-

side Cs corrector. X-ray powder diffraction (XRD) patterns were obtained with a high power X-ray diffractometer (Rigaku) equipped with Cu  $K_{\alpha}$  radiation, operated at 40 kV and 200 mA. XRD patterns were measured in a  $2\theta$  range from  $10^{\circ}$  to  $90^{\circ}$  with a scan rate of  $4^{\circ} \text{ min}^{-1}$ . The chemical states of the samples were analyzed using an X-ray photoelectron spectrometer (XPS, K-alpha, ThermoScientific) equipped with a monochromatic Al  $K_{\alpha}$  X-ray source (1486.6 eV). The oxidation state of the samples was investigated using X-ray absorption near edge spectroscopy (XANES) analysis, performed on a Beamline 10C from the Pohang Accelerator Laboratory (PAL) in South Korea, with beam energy of 3 GeV and current of 280 mA. X-ray photon energy was monochromatized by a Si(1 1 1) double-crystal monochromator, which was detuned by approximately 30% to remove high-order harmonics. Data for W  $L_{1-}$  and W  $L_{3-}$  edge XANES spectra were taken at room temperature (RT) using a fluorescence detector.

### 1.3. Electrochemical Measurements

All electrochemical measurements were performed on an IviumStat electrochemical analyzer at RT and atmospheric pressure, using a three-compartment electrochemical cell. A graphite rod was used as the counter electrode, with Ag/AgCl (in 3 M NaCl solution) as the reference electrode. The Ag/AgCl reference electrode was calibrated with respect to the reversible hydrogen electrode (RHE) before every use. For the calibration, the hydrogen reference electrode (Hydroflex<sup>®</sup>, Gaskatel) and the Ag/AgCl electrode were immersed in a 0.5 M  $\text{H}_2\text{SO}_4$  solution for 30 min. The open circuit voltage (OCV) was recorded for use in the following calculation:  $E(\text{RHE}) = E(\text{Ag/AgCl}) - \text{OCV}$ . All potentials quoted in this study are presented on the RHE scale. For electrochemical measurements, a rotating disk electrode (RDE) containing a glassy carbon (GC) central disk (4-mm diameter,  $0.126\text{-cm}^2$  area) was used as the working electrode. The RDE was polished with a  $1.0\text{-}\mu\text{m}$  alumina suspension, followed by a  $0.3\text{-}\mu\text{m}$  suspension to generate a mirror finish before use. Catalyst inks were prepared by mixing catalyst (8 mg) with Nafion (80  $\mu\text{L}$ , 5 wt% in isopropanol, Sigma-Aldrich) in a solution of DI water (800  $\mu\text{L}$ ) and EtOH (200  $\mu\text{L}$ , 99.9%), and the mixture was sonicated for 30 min to give an homogeneous slurry. A sample of the catalyst ink (5  $\mu\text{L}$ ) was then dropped onto the glassy carbon electrode, and dried at RT for 30 min, with a rotation speed of 700 rpm. The resulting catalyst loading on the GC disc was calculated to be  $300 \mu\text{g}\cdot\text{cm}^{-2}$ . Before electrochemical measurements were taken, a stream of  $\text{N}_2$  was bubbled through the 0.5 M  $\text{H}_2\text{SO}_4$  electrolyte solution for 20 min. Cyclic voltammetry (CV) was then carried out for

electrochemical activation, which consisted of 20 repetitions in a potential range of 0.05 to 1.2 V (vs. RHE) at a scan rate of 100 mV s<sup>-1</sup>. Linear sweep voltammetry (LSV) for the hydrogen evolution reaction (HER) was conducted from 0.1 V to -0.4 V (vs. RHE) at a scan rate of 2 mV s<sup>-1</sup> with a rotating speed of 1500 rpm in a 0.5 M H<sub>2</sub>SO<sub>4</sub> solution, continuously purged with H<sub>2</sub> gas. Electrochemical impedance spectroscopy (EIS) was performed on the same electrochemical system. After electrochemical activation by CV, the Nyquist plots were observed in a frequency range of 100 kHz to 0.01 Hz at an overpotential of 100 mV.

## 2. Supplementary Figures S1-S4

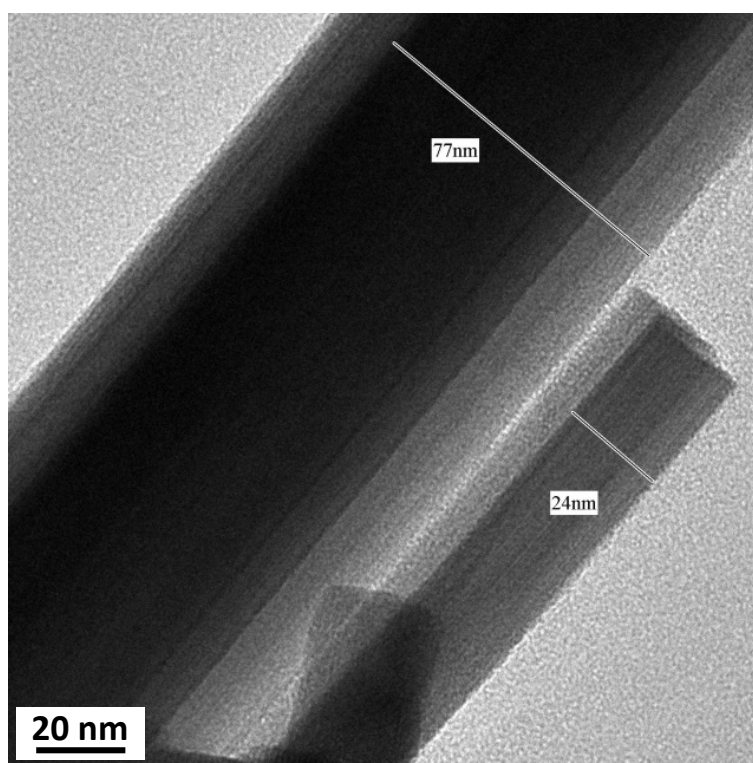


**Fig. S1** Suboxide (W<sub>18</sub>O<sub>49</sub>) whiskers after reaction for a few min (no sulfide layers observed).

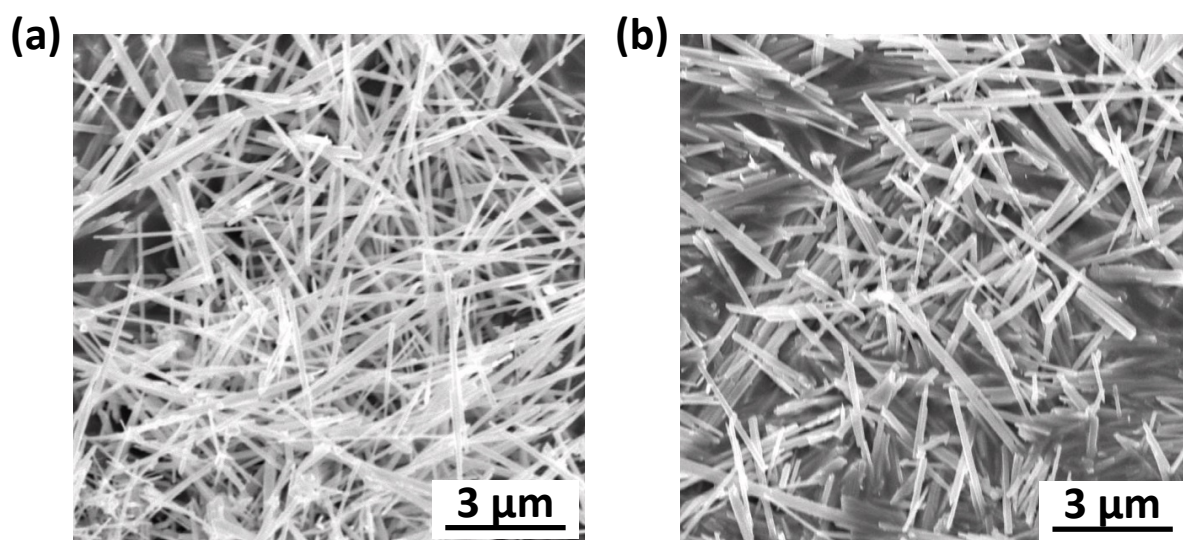


**Fig. S2** SEM images of (a) WS<sub>2</sub> NTs and (b) W<sub>18</sub>O<sub>49</sub>@WS<sub>2</sub> NRs.

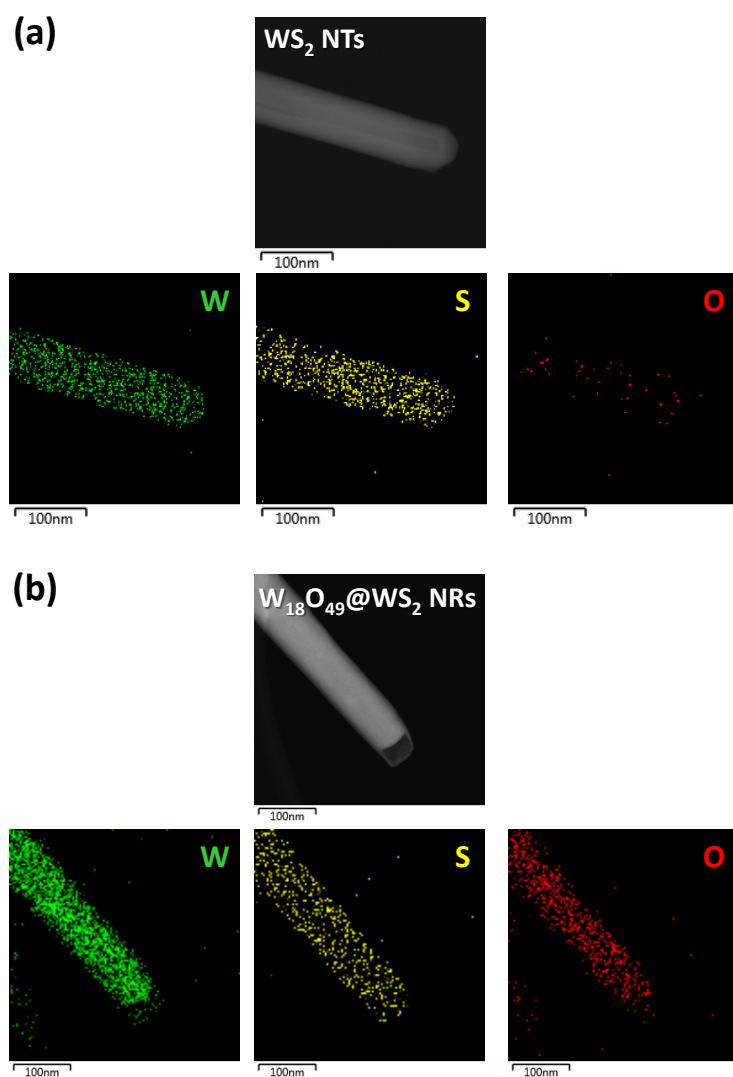


**Fig. S3** EDX elemental mapping images of (a) WS<sub>2</sub> NTs and (b) W<sub>18</sub>O<sub>49</sub>@WS<sub>2</sub> NRs.

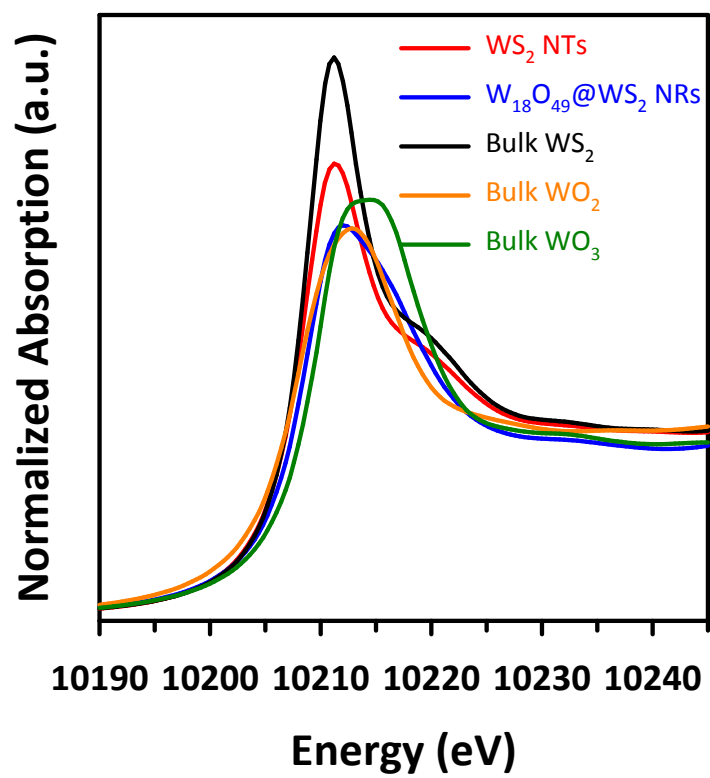


**Fig. S4** W L<sub>3</sub>-edge XANES spectra



### 3. References for Electronic Supplementary Information

- S1. A. Rothschild, J. Sloan, and R. Tenne, *J. Am. Chem. Soc.* 2000, **122**, 5169-5179.
- S2. A. Zak, L. Sallacan-Ecker, A. Margolin, Y. Feldman, R. Popovitz-Biro, A. Albu-Yaron, M. Genut, and R. Tenne, *Fullerene, Nanotubes, Carbon Nanostruct.* 2011, **19**, 18-26.